Geometric Analysis of Multivariable Control Systems
M.L. Nagurka, T.R. Kurfess
EDRC 24-83-92

Geometric Analysis of Multivariable Control Systems

M.L. Nagurka and **T.R. Kurfess**
Department of Mechanical Engineering
Carnegie Mellon University
Pittsburgh, PA 15213

March 1992

This report promotes a new graphical representation of the behavior of linear, time-invariant, multivariable systems highly suited for exploring the influence of closed-loop system parameters. The development is based on the adjustment of a scalar control gain cascaded with a square multivariable plant embedded in an output feedback configuration. By tracking the closed–loop eigenvalues as an explicit function of gain, it is possible to visualize the multivariable root loci in a set of "gain plots" consisting of two graphs: (i) magnitude of system eigenvalues vs. gain, and (ii) argument (angle) of system eigenvalues vs. gain. By depicting unambiguously the polar coordinates of each eigenvalue in the complex plane, the gain plots complement the standard multi-input, multi-output root locus plot. Two example problems demonstrate the utility of gain plots for interpreting linear multivariable system behavior.

Introduction

Since their introduction, classical controls tools have been popular for analysis and design of single–input, single–output (SISO) systems. These methods may be viewed as specialized versions of more general tools that are applicable to multi–input, multi–output (MIMO) systems. Although modern "state–space" control methods (relying on dynamic models of internal structure) are generally promoted as the predominant tools for multivariable system analysis, the classical control extensions offer several advantages, including requiring only an input–output map and providing direct insight into stability, performance, and robustness of MIMO systems. The understanding generated by these graphically–based methods for the analysis and design of MIMO systems is a prime motivator of this research.

An early graphical method for investigating the stability of linear, time–invariant (LTI) SISO systems was developed by Nyquist (1932) and is based on a polar plot of the loop transmission transfer function. The MIMO analog of the Nyquist diagram is the multivariable Nyquist diagram which is used in conjunction with the corresponding multivariable Nyquist criterion (Rosenbrock, 1974; Lehtomaki, *et al.*, 1981; Friedland, 1986). This criterion is complicated in the MIMO case because it is expressed in terms of the determinant of the return difference transfer function matrix ([I + G(s)] where G(s) is the plant transfer function matrix, rather than just 1 + g(s) for the SISO case where g(s) is the plant transfer function). Despite the complication, significant research has supported the MIMO Nyquist extension for assessment of multivariable system stability and robustness (MacFarlane and Postlethwaite, 1977).

The Bode plots (Bode, 1940) recast the information of the Nyquist diagram, with frequency extracted as an explicit parameter. The MIMO analog or extension of the classical Bode magnitude plot is the singular value Bode–type plot that shows maximum and minimum singular values of transfer function matrices as a function of frequency (Doyle and Stein, 1981). This generalized magnitude *vs.* frequency plot is useful for analysis, providing performance insight in terms of command following, disturbance rejection, and sensor noise sensitivity, as well as for design, in terms of frequency shaping (Doyle and Stein, 1981; Safanov, *et al.*, 1981; Athans, 1982; Maciejowski, 1989).

Although promoted as an SISO tool, Evans root locus method (Evans, 1954) is also extendable to MIMO systems, since it depicts the trajectories of closed–loop eigenvalues (of either SISO or MIMO systems) in a complex plane. However, the generalization to the multivariable root loci has not made as significant an impact as the

1

MIMO versions of the classical frequency-domain tools. In similarity to the multivariable Nyquist diagram and Bode plot, the MIMO root locus plot does not, in general, follow the straight-forward sketching rules applicable to SISO systems. However, it does provide insight into stability and performance of the closed-loop system. Part of the complication of the MIMO root locus relates to the fact that "multivariable root loci live on a Riemann surface ... as compared with the single-input, single-output case where the root loci lie on a simple complex plane (a trivial, *i.e.*, one sheeted, Riemann surface)" (Postlethwaite and MacFarlane, 1979). As a result, multivariable root loci tend to have strange looking patterns when drawn in a single complex plane. The possibility of loci being multi-valued functions of gain can make the MIMO root locus plot somewhat confusing.

To aid the controls engineer in extracting more information from the multivariable Evans root locus plot, we propose a set of "gain plots" that provide a direct and unique window into the stability, performance, and robustness of LTI MIMO systems. A conceptual framework motivating the gain plots and a discussion of their applicability to SISO systems has been presented previously (Kurfess and Nagurka, 1991a).

Multivariable Eigenvalue Description

Review of Basic MIMO Concepts

A LTI MIMO system can be represented in the standard state-space form as

$$\dot{x}(t) = A x(t) + B u(t) \qquad (1)$$

$$y(t) = C x(t) + D u(t) \qquad (2)$$

where state vector x is length n, control input vector u is length m, and output vector y is length, m. Matrices A, B, C and D are the system matrix, the control influence matrix, the output matrix, and the feed-forward matrix, respectively, with appropriate dimensions. The input-output dynamics are governed by a square transfer function matrix, G(s),

$$G(s) = C[sI - A]^{-1}B + D \qquad (3)$$

The system is embedded in the closed-loop configuration, shown in Figure 1, where the controller is a static compensator, kI, implying that each input channel is scaled by the same constant gain k. (Note that the plant transfer function matrix and any dynamic compensation may be combined in the transfer function matrix G(s).) The control law is given by

2

$$u(t) = k\,\mathbf{I}\,e(t) \tag{4}$$

where

$$e(t) = r(t) - y(t) \tag{5}$$

is the error and $r(t)$ is the reference (command) signal vector of length m that $y(t)$ must track. The closed–loop transfer function matrix is

$$G_{CL}(s) = [\,\mathbf{I} + k\,G(s)\,]^{-1} k\,G(s) \tag{6}$$

In the MIMO root locus plot, the migration of the eigenvalues of $G_{CL}(s)$ in the complex plane is graphed as scalar k varies in the range $0 \le k < \infty$. The eigenvalues of the closed–loop system, $s = \lambda_i$ ($i=1,2,\dots,n$), are the roots of $\phi_{CL}(s)$, the closed–loop characteristic polynomial,

$$\phi_{CL}(s) = \phi_{OL}(s)\,\det[\mathbf{I} + k\,G(s)] \tag{7}$$

where $\phi_{OL}(s)$ is the open–loop characteristic polynomial,

$$\phi_{OL}(s) = \det[s\,\mathbf{I} - A] \tag{8}$$

The roots, or solutions of equation (8), are the open–loop poles. By equating the determinant in equation (7) to zero, the MIMO generalization of the SISO characteristic equation $\{1 + kg(s) = 0\}$ is obtained. The presence of the determinant is the major challenge in generalizing the SISO root locus sketching rules to MIMO systems and complicates the root locus plot. For example, the root locus branches "move" between several copies (Riemann sheets) in the s–plane that are connected at singularity points known as branch points (Yagle, 1981; Athans, 1982).

Although it is not generally possible to sketch MIMO root loci by inspection, the closed–loop system eigenvalues may be computed numerically from equations (1) – (5) as

$$\lambda_i = \mathrm{eig}\big[A - B(\mathbf{I} + kD)^{-1}kC\big]\,, \quad i = 1, 2, \cdots, n \tag{9}$$

In the examples, the loci of the eigenvalues are calculated from equation (9) as k is monotonically increased from zero.

High Gain Behavior

As the gain increases from zero to infinity, the closed–loop eigenvalues trace out "root loci" in the complex plane. At zero gain, the poles of the closed–loop system are the

3

open–loop eigenvalues. At infinite gain some of the eigenvalues approach finite transmission zeros, defined to be those values of s that satisfy the generalized eigenvalue problem

$$\begin{bmatrix} s\,I - A & -B \\ C & D \end{bmatrix}\begin{bmatrix} x(0) \\ u \end{bmatrix} = \begin{bmatrix} 0 \\ 0 \end{bmatrix} \qquad (10)$$

where $[\ x(0)\ u\ ]^T$ is the right generalized eigenvector corresponding to the generalized eigenvalue, *i.e.*, transmission zero, with $x(0)$ representing the initial state and u being a vector representing input direction in the multi–input case. In the absence of pole/zero cancellation, the finite transmission zeros are the roots of the determinant of $G(s)$. Algorithms have been developed for efficient and accurate computation of transmission zeros (Davison and Wang, 1974; Laub and Moore, 1978; Westreich, 1991).

The high gain behavior of the root loci can be viewed another way (Friedland, 1986). The eigenvalues can be considered as always migrating from the open–loop poles to their matching transmission zeros. However, those eigenvalues that do not have matching zeros in the finite part of the s–plane are considered to have matching zeros at infinity. In the global SISO perspective, whenever there exists an excess of poles over zeros, the eigenvalues migrate towards infinity in a Butterworth configuration. If the excess of poles over zeros is greater than two for an SISO system the closed–loop eigenvalues must become unstable as $k \rightarrow \infty$. A single Butterworth configuration at high gain is generally not seen in the MIMO case; rather, multiple Butterworth configurations are generated. It can be shown that for a square system with m inputs, m outputs, and m or more eigenvalues migrating towards infinity, m high gain Butterworth patterns occur (Kwakernaak, 1976; Shaked, 1978, Thompson, *et. al.*, 1982). These patterns do not necessarily demonstrate some of the properties of the well known SISO Butterworth configurations, such as the angle criterion or a center of gravity on the real axis. The MIMO Butterworth patterns do, however, reveal the typical Butterworth magnitude characteristic that has been demonstrated for SISO systems (Kurfess and Nagurka, 1991b). These features are shown later via example.

MIMO Gain Plots

Just as the Bode plots embellish the information of the Nyquist diagram by exposing frequency explicitly in a set of magnitude *vs.* frequency and angle (phase) *vs.* frequency plots, it follows that a pair of gain plots (Kurfess and Nagurka, 1991a) can enhance the standard root locus plot. As the gain-domain analog of the frequency-domain Bode plots, the gain plots explicitly graph the eigenvalue magnitude *vs.* gain in a magnitude

gain plot, and the eigenvalue angle *vs.* gain in an angle gain plot. In similarity to the Bode plots, the magnitude gain plot employs a log-log scale whereas the angle gain plot uses a semi-log scale (with the logarithms being base 10). Although gain is selected as the variable of interest in the gain plots, it should be noted that any scalar parameter may be used in the geometric analysis.

Gain plots can be drawn for both SISO and MIMO systems. In MIMO systems it is assumed that the compensation dynamics are governed by a single scalar gain amplifying all plant inputs. For such systems, simultaneous inspection of the magnitude and angle gain plots enables one to uniquely identify locus branches as a function of gain. As such, gain plots are a natural complement to multivariable root locus plots, where uncharacteristically confusing eigenvalue trajectories can result from being drawn in a single complex plane.

MIMO Examples

This section presents two multivariable examples. The first example is designed to introduce the concept of the gain plots, and to demonstrate the insight they offer by "unwrapping" the multivariable root locus and exposing unambiguous behavior. The second example highlights the power of the gain plots in revealing typical multivariable properties, such as high gain Butterworth patterns for both magnitude and angle.

Example 1: Aircraft Vertical Plane Dynamics

The state space model (from Hung and MacFarlane (1982) and studied in detail by Maciejowski (1989)),

$$\dot{x} = \begin{bmatrix} 0 & 0 & 1.132 & 0 & -1 \\ 0 & -0.054 & -0.171 & 0 & 0.071 \\ 0 & 0 & 0 & 1 & 0 \\ 0 & 0.049 & 0 & -0.856 & -1.013 \\ 0 & -0.291 & 0 & 1.053 & -0.686 \end{bmatrix} x + \begin{bmatrix} 0 & 0 & 0 \\ -0.120 & 1 & 0 \\ 0 & 0 & 0 \\ 4.419 & 0 & -1.665 \\ 1.575 & 0 & -0.073 \end{bmatrix} u \quad (11)$$

$$y = \begin{bmatrix} 1 & 0 & 0 & 0 & 0 \\ 0 & 1 & 0 & 0 & 0 \\ 0 & 0 & 1 & 0 & 0 \end{bmatrix} x \quad (12)$$

represents a linearized model of the vertical plane dynamics of an aircraft. The system, with three inputs, three outputs and five state variables, has no finite transmission zeros and has open-loop eigenvalues of $\lambda_i = \{0, -0.7801 \pm 1.0296j, -0.0176 \pm 0.1826j\}$. The eigenvalue at the origin indicates that the open-loop system is marginally stable. The

trajectories of the closed–loop system eigenvalues may be graphically displayed in the MIMO root locus shown in Figure 2. However, it is not clear if there exist gains for which all of the eigenvalues reside in the left–half plane, implying that the system can be stabilized for certain gains. The MIMO root locus plot suggests that as the gain is raised the system becomes unstable, but fails to indicate the gain at which instability occurs. Closer inspection of the eigenvalues indicates that the closed–loop system is never stable for positive gains.

The gain plots for this system, shown in Figure 3a,b, reveal this information about the closed–loop system instability. For example, they show that as the gain increases the eigenvalue at the origin initially migrates along the positive real axis (*i.e.*, $\angle s = 0°$), indicating instability, until it reaches a maximum value of s≈0.010 at a gain k≈0.018. As the gain increases, this real eigenvalue reverses direction, crosses the imaginary axis at a gain k≈0.043, and continues to move along the negative real axis (*i.e.*, $\angle s = 180°$). However, at k≈0.043 one pair of complex conjugate eigenvalues has already moved into the right half plane (crossing the imaginary axis at a slightly lower gain). The angle gain plot of Figure 3b shows this behavior clearly. In summary, the gain plots provide an unambiguous means by which stability may be determined.

The gain plots highlight several other important features. For example, they show the gains corresponding to the complex conjugate eigenvalue pairs breaking into the real axis and then proceeding to ±∞. Complex conjugate eigenvalues are shown as symmetric lines about either the 180° or 0° line with equal magnitudes. Purely real eigenvalues possess equal angles (180° or 0°) but distinct magnitudes. This behavior is demonstrated in Figure 3a,b, from which the gains at the breakpoints may be determined by inspection.

The rates at which the eigenvalues increase towards a magnitude of infinity is seen in the magnitude gain plot of Figure 3a and in expanded form in Figure 4. The single eigenvalue that begins at the origin proceeds towards infinity along the negative real axis at a rate proportional to k (the high gain magnitude gain plot slope is unity). This slope is characteristic of a first order Butterworth pattern. The two complex conjugate eigenvalue pairs proceed toward infinity at a rate proportional to $k^{1/2}$ (shown as a high gain magnitude gain plot slope of 1/2), indicative of a second order Butterworth pattern (Kurfess and Nagurka, 1991b).

From Figure 4, the two complex conjugate eigenvalue pairs at high gains have slope values of 1/2. As k→∞, this group of four parallel lines separates into two co–linear sets. An interesting fact is that the two identical lines are comprised of an eigenvalue

6

magnitude from each of the original complex conjugate pairs. It is as if the complex conjugate eigenvalues have *swapped partners*. This phenomenon is not apparent from the MIMO root locus; however, it must occur due to the location of the centers of gravity for the two second order Butterworth patterns. In fact, each set of co-linear trajectories represents a Butterworth configuration.

Example 2: Higher Order System with Feedforward Term

This example, from (Kouvaritakis and Edmunds, 1979), demonstrates the power of the gain plot geometry in exposing multivariable system behavior. It represents a three input, three output, seventh order system with three transmission zeros. The system is given by the state space representation of equations (1) and (2) where

$$A = \frac{1}{16} \begin{bmatrix} -32 & -80 & 16 & 0 & 0 & 0 & 0 \\ 16 & -64 & -16 & 0 & 0 & 0 & 0 \\ 0 & 0 & -48 & 0 & 0 & 0 & 0 \\ 0 & 0 & 0 & -32 & -80 & 0 & 0 \\ 0 & 0 & 0 & 16 & -64 & 0 & 0 \\ 1653 & 0 & 0 & 3424 & 0 & -32 & -80 \\ 76 & 0 & 0 & 928 & 0 & 16 & -64 \end{bmatrix} \tag{13}$$

$$B = \begin{bmatrix} 1 & 0 & 0 \\ -1 & 2 & -2 \\ 1 & 1 & 2 \\ 0 & 1 & 0 \\ 0 & 0 & 1 \\ 0 & 0 & 0 \\ 0 & 0 & 0 \end{bmatrix} \tag{14}$$

$$C = \frac{1}{16} \begin{bmatrix} 8 & -16 & 0 & 0 & 0 & 0 & 0 \\ -8 & -8 & 16 & -15 & -37 & 8 & 0 \\ 0 & 8 & 16 & -68 & 36 & 0 & 8 \end{bmatrix} \tag{15}$$

$$D = \begin{bmatrix} -8 & -2 & 10 \\ -4 & -1 & 5 \\ -8 & -2 & 10 \end{bmatrix} \tag{16}$$

The system is somewhat unusual due to the presence of the feedforward term (*i.e.*, the D matrix is non-zero). The root locus plot for this system is shown in Figure 5, and the multivariable gain plots for the system are depicted in Figures 6a,b.

From the root locus and gain plots, it is clear that there are three sets of complex conjugate open-loop eigenvalues at $s = -3 \pm 2j$, and a single real open-loop eigenvalue at s

= –3. There is also a set of complex conjugate multivariable transmission zeros s ≈ –2.84 ± 1.31j and a real zero at s ≈ –124. As the control configuration of Figure 1 is employed, the real eigenvalue moves first in the negative direction and then in the positive direction along the real axis. Inspection of the gain plots shows that the real eigenvalue reaches a maximum value of approximately –2.5 at a gain of approximately 0.1. The eigenvalue then branches to a different Riemann sheet and traverses along the real axis towards the real transmission zero. By inspection of the gain plots, pole/zero cancellation for the real zero occurs at $k \approx 10^4$.

A set of complex conjugate eigenvalues moves towards the transmission zeros as the gain is increased. The remaining two sets of eigenvalue pairs travel towards infinity in two separate second order Butterworth configurations. By inspection of the gain plots, pole/zero cancellation for the complex conjugate zeros occurs at a gain $k \approx 10^0$.

To further highlight the enriched perspective offered by the gain plots, a MIMO root locus plot for higher gain values is shown in Figure 7. (Because of the logarithmic scales used in the gain plots, expanded high gain plots are not necessary.) From Figure 7 the Butterworth patterns may not be clearly visible, yet from Figures 6a,b two distinct patterns arise. From the magnitude gain plot, the two separate configurations may be separated into two second order patterns having slopes of 1/2 (Kurfess and Nagurka, 1991b).

Further insight into the different patterns is available from the information of the gain plots. Although there are two sets of complex conjugate eigenvalues, the Butterworth patterns are formed from one eigenvalue of each complex set. This is demonstrated in both the magnitude and angle gain plots. The angles of the complex conjugate eigenvalues are approximately ±115° and ±65°. Thus, each member complex pair is approximately 180° in angular distance from its matching Butterworth partner in the other complex pair. From simple geometric relationships, the centers of gravity (sometimes referred to as pivots) from the two second order Butterworth patterns may be computed to be approximately 19.2±11.9j (Wang, *et al.*, 1991).

Conclusions

In typical MIMO root locus plots trajectories may be camouflaged as some branches may overlap. Gain plots are promoted as a means to "untangle" MIMO eigenvalue trajectories. The major enhancement is the visualization of eigenvalue trajectories as an c :plicit function of gain (where the compensation has been assumed to be the same static

gain applied to all control channels). The representation provides a unique description of the eigenvalues and their trajectories as a parameter, such as gain, is varied.

Research efforts, currently underway, may shed additional light on gain plots for multivariable systems. In addition, work by MacFarlane and Postlethwaite (1977, 1979) and Hung and MacFarlane (1982) on relating characteristic frequency plots to gain domain geometry promises closer connections between gain plot methods and singular value frequency methods.

In conclusion, gain plots enrich the multivariable root locus plot in much the same way that singular value frequency plots are an alternate and extended presentation of the multivariable Nyquist diagram. Their use in conjunction with the multivariable root locus provides a new geometric perspective on multivariable systems that can result in clearer understandings of such systems in both the research and teaching realms of control engineering.

Acknowledgement

The authors wish to thank Mr. Ssu-Kuei Wang for his help, and for his earnest enthusiasm of gain plots for studying multivariable and optimal systems.

References

Athans, M., 1982, "Lecture Notes on Multivariable Control Systems: MIT Subject 6.232," Massachusetts Institute of Technology, Cambridge, MA.

Bode, H. W., 1940, "Relations Between Attenuation and Phase in Feedback Amplifier Design," Bell System Technical Journal, vol. 19, pp 421–454.

Davison, E.J. and Wang, S.H., 1974, "Properties and Calculation of Transmission Zeros of Linear Multivariable Systems," Automatica, vol. 10, pp 643–658.

Evans, W. R., 1954, Control System Dynamics, McGraw–Hill, New York.

Friedland, B., 1986, Control System Design, McGraw–Hill, New York.

Hung, Y. S. and MacFarlane, A. G. J., 1982, Multivariable Feedback: A Quasi–Classical Approach, Lecture Notes in Control and Information Sciences, vol. 40, Springer–Verlag, Berlin.

Kurfess, T. R. and Nagurka, M. L., 1991a, "A New Visualization of the Evans Root Locus: Gain Plots," DSC–Vol. 27, Robust Control of Mechanical Systems: Theory and Applications, Winter Annual Meeting, American Society of Mechanical Engineers, Atlanta, GA, December, pp 1–8.

Kurfess, T. R. and Nagurka, M. L., 1991b, "High Gain Control System Design with Gain Plots," Technical Report #EDRC 24-48-91, Engineering Design Research Center, Carnegie Mellon University, Pittsburgh, PA.

Kwakernaak, H., 1976 "Asymptotic Root Loci of Multivariable Linear Optimal Regulators," IEEE Transactions on Automatic Control, vol. AC-21, no. 3, pp 378-382.

Laub, A. J. and Moore, B. C., 1978, "Calculation of Transmission Zeros Using QZ Techniques," Automatica, vol. 14, no. 6, pp 557-566.

Lehtomaki, N. A., Sandell, N.R. Jr., and Athans, M., 1981, "Robustness Results in Linear-Quadratic Gaussian Based Multivariable Control Designs," IEEE Transactions on Automatic Control, vol. AC-26, no. 1, pp 75-93.

Maciejowski, J. M., 1989, Multivariable Feedback Design, Addison-Wesley Publishing Co., Reading, MA.

MacFarlane A. G. J. and Postlethwaite, I., 1977, "The Generalized Nyquist Stability Criterion and Multivariable Root Loci," International Journal of Control, vol. 25, pp 81-127.

Nyquist, H., 1932, "Regeneration Theory," Bell System Technical Journal, vol. 11, pp 126-147.

Postlethwaite, I. and MacFarlane A. G. J., 1979, A Complex Variable Approach to the Analysis of Linear Multivariable Feedback Systems, Lecture Notes in Control and Information Science, Springer-Verlag, New York, NY.

Rosenbrock, H.H., 1974, Computer-Aided Control System Design, Academic Press, London.

Safanov, M.G., Laub, A.J., and Hartmann, G.L., 1981, "Feedback Properties of Multivariable Systems: The Role and Use of the Return Difference Matrix," IEEE Transactions on Automatic Control, vol. AC-26, no. 1, pp 47-65.

Shaked, U., 1978, "The Asymptotic Behavior of Multivariable Optimal Regulators," IEEE Transactions on Automatic Control, vol. AC-23, no. 3, pp 425-430.

Thompson, P. M., Stein, G., and Laub, A. J., 1982, "Angles of Multivariable Root Loci," IEEE Transactions on Automatic Control, vol AC-27, no. 6, pp 1241-1243.

Wang, S. K., Nagurka, M. L., and Kurfess, T. R., "Asymptotic Behavior of Optimal Root Loci," Technical Report #EDRC 24-79-92, Engineering Design Research Center, Carnegie Mellon University, Pittsburgh, PA, 1991.

Westreich, D., 1991, "Computing Transfer Function Zeros of a State Space System," International Journal of Control, vol. 53, No. 2, pp 477-493.

Yagle, A.E., 1981, Properties of Multivariable Root Loci, S.M. Thesis, Department of Electrical Engineering and Computer Science, Massachusetts Institute of Technology, Cambridge, MA.

Figure Captions

Figure 1.   MIMO Closed-Loop Negative Feedback Configuration.

Figure 2.   Root Locus Plot of Example 1.

Figure 3.   (a) Magnitude and (b) Angle Gain Plots of Example 1.

Figure 4.   Expanded Magnitude Gain Plot of Example 1.

Figure 5.   Root Locus Plot of Example 2.

Figure 6.   (a) Magnitude and (b) Angle Gain Plots of Example 2.

Figure 7.   Expanded Range Root Locus Plot of Example 2.
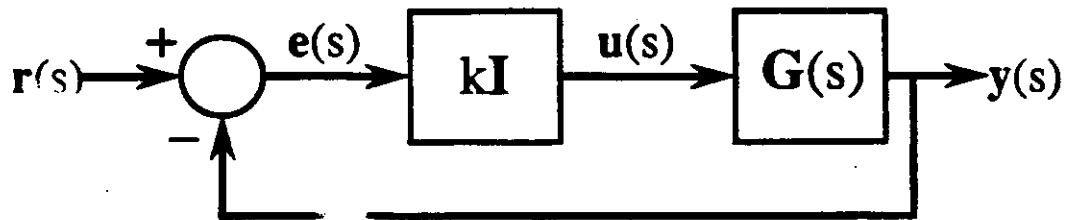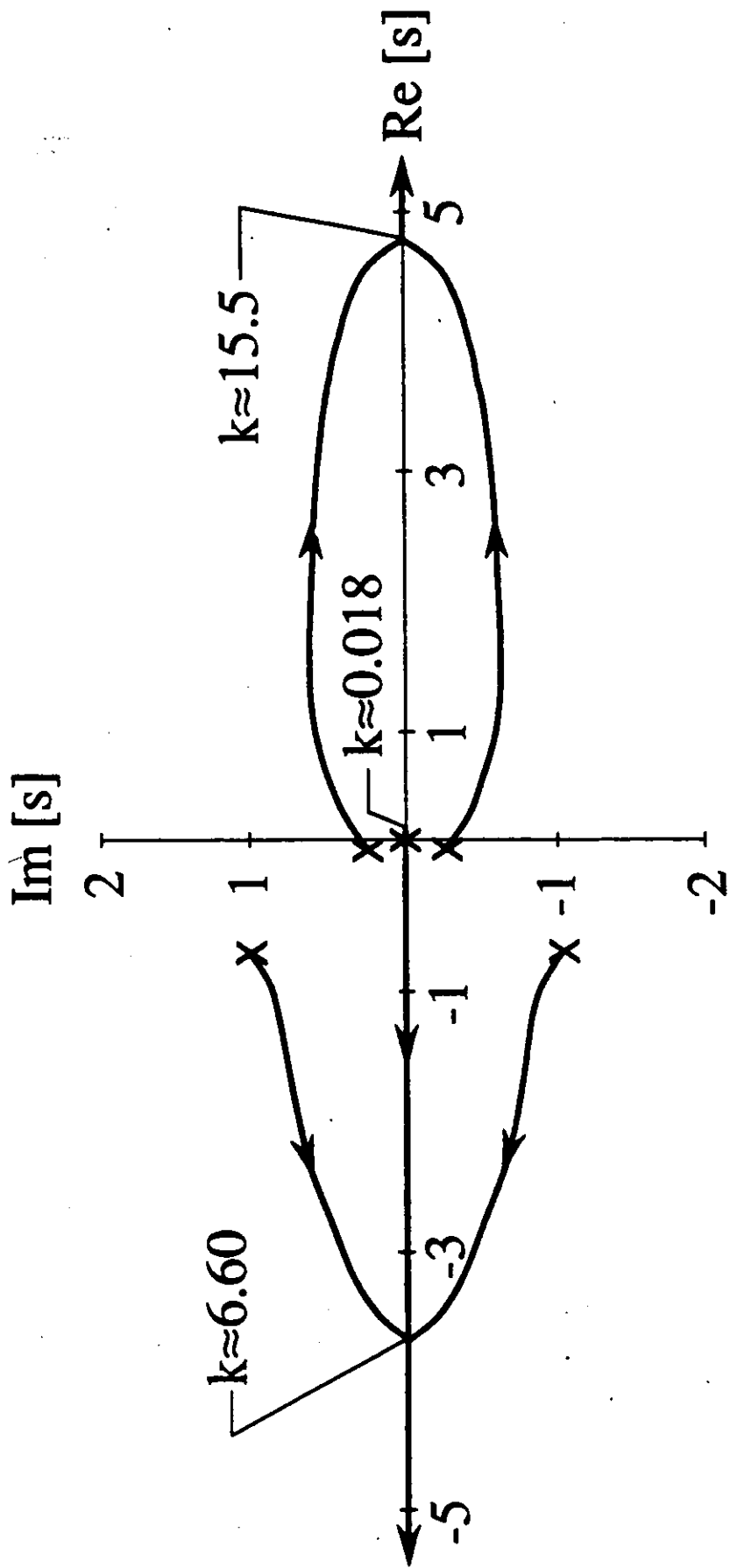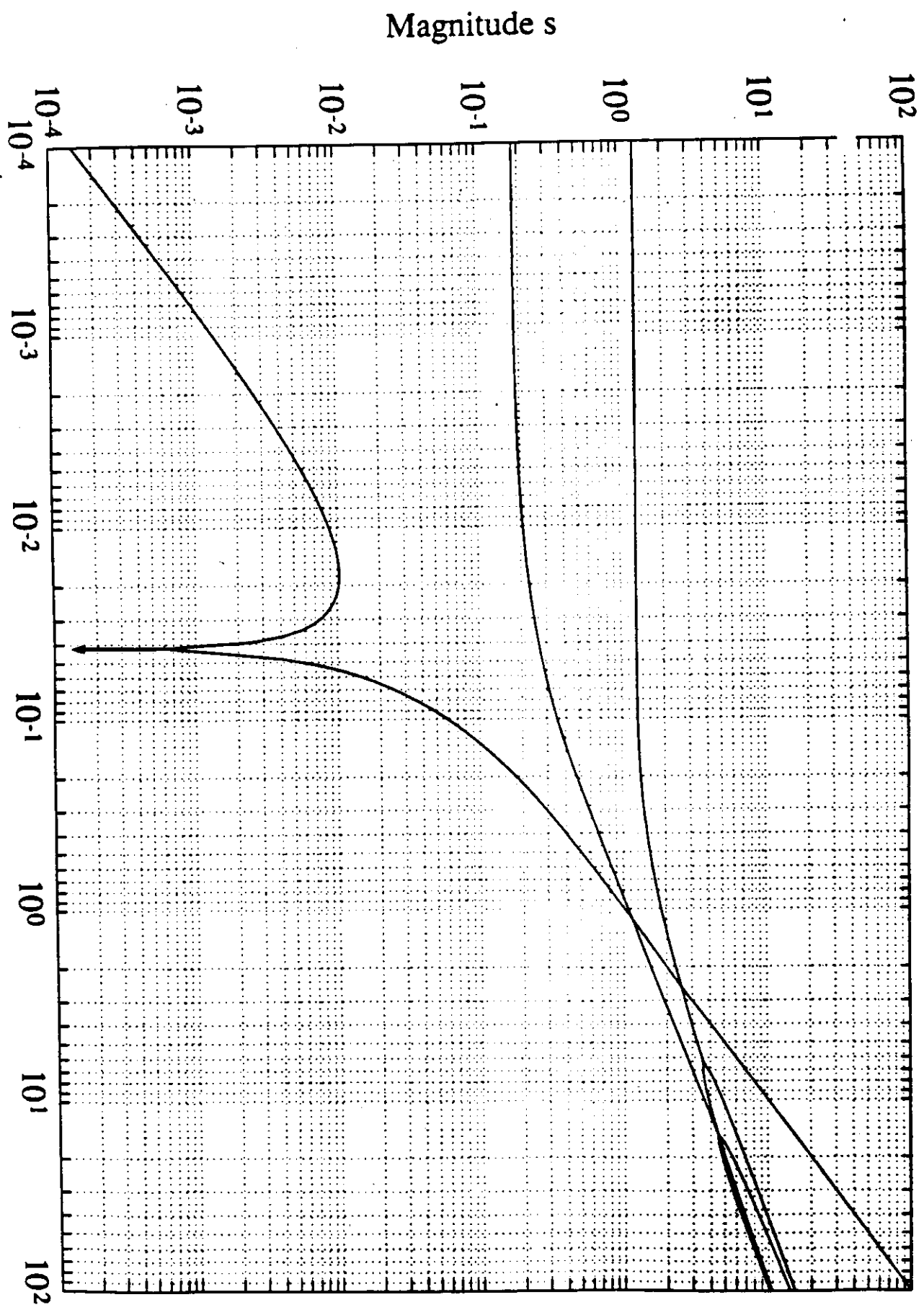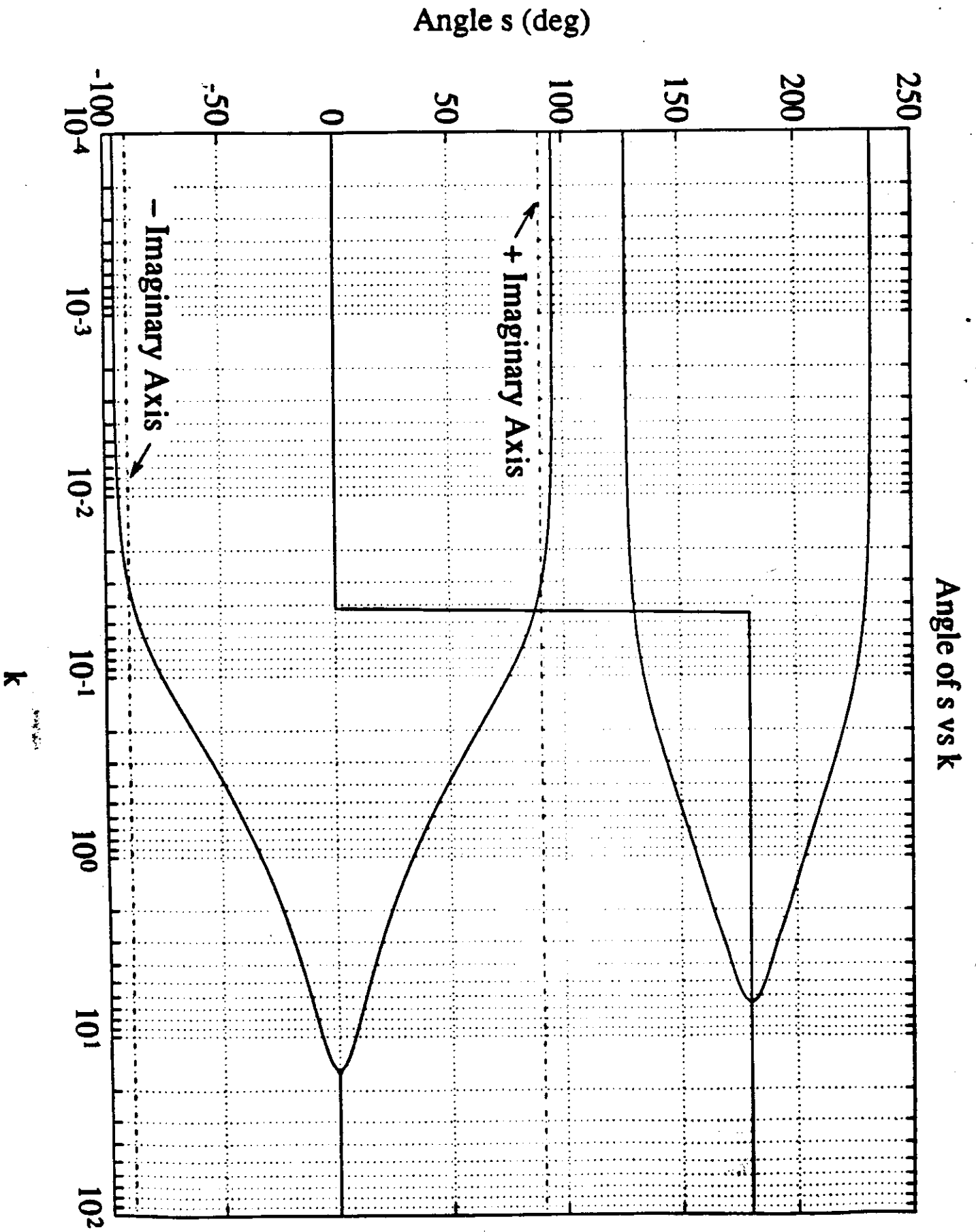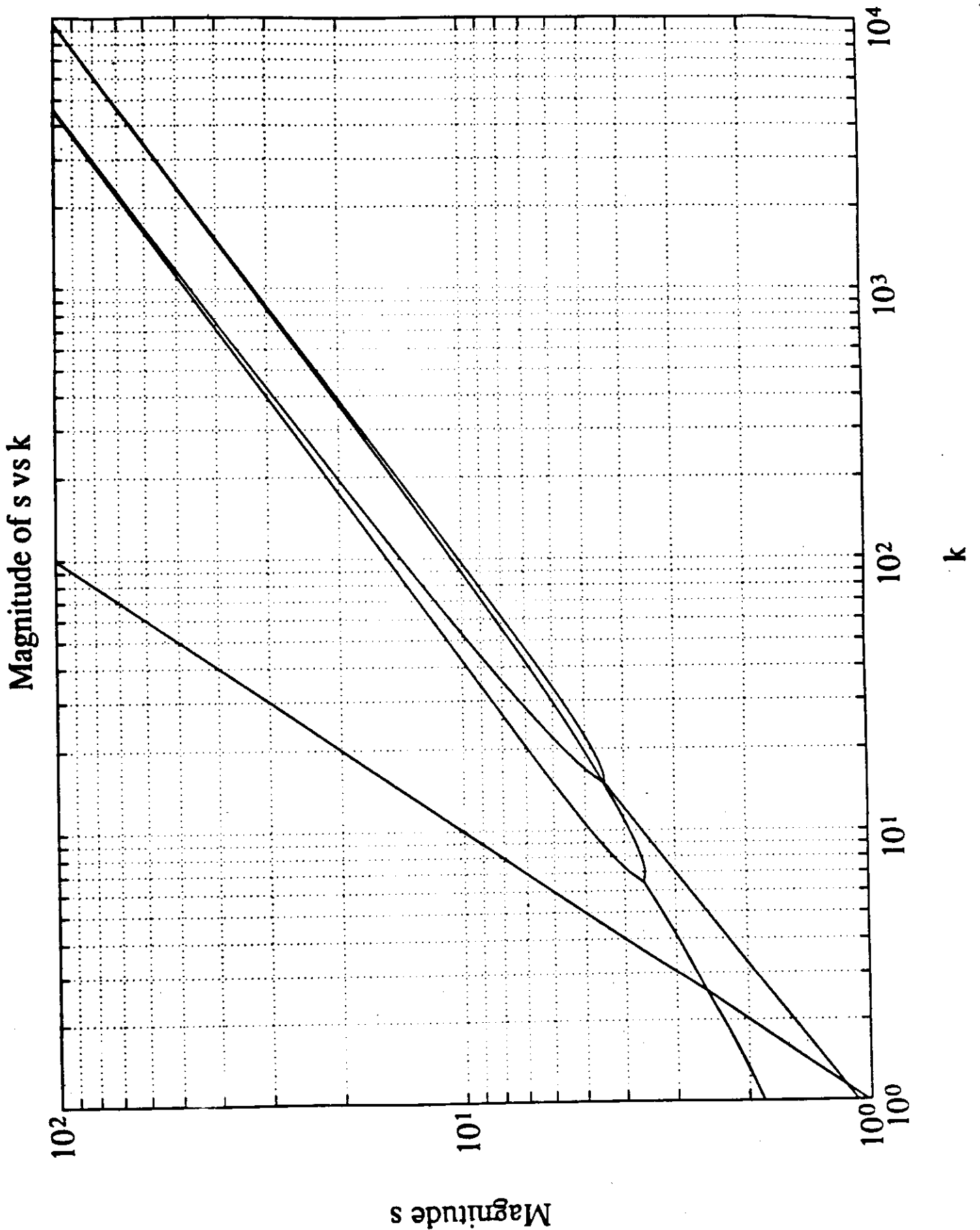
Figure 1. MIMO Closed–Loop Negative Feedback Configuration.

Figure 2.

Magnitude of s vs k

Magnitude s

k

Angle of s vs k

Angle s (deg)

+ Imaginary Axis

− Imaginary Axis

k

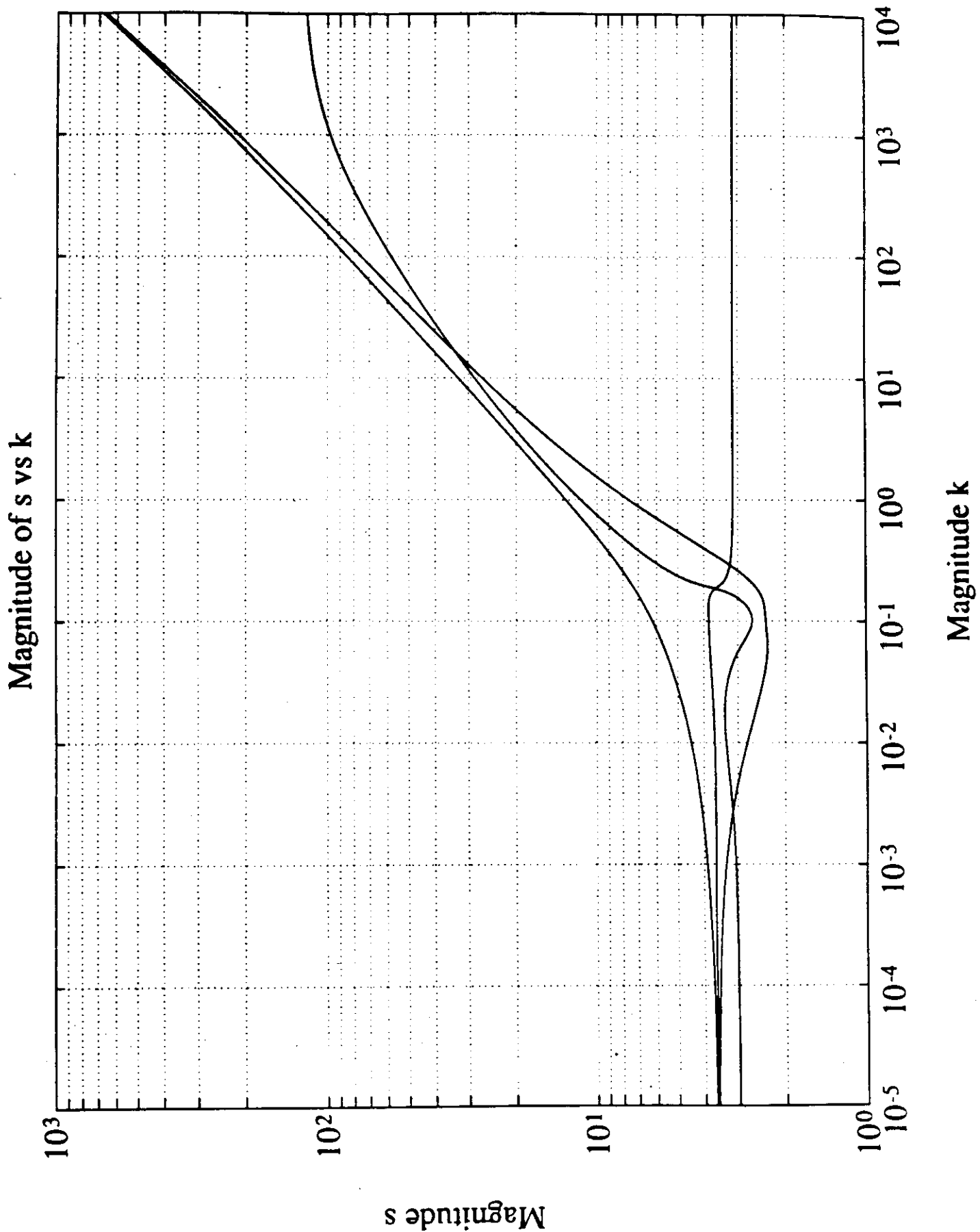Magnitude of s vs k

k

Magnitude s

Real s

Imag s

FIG 5

Magnitude of s vs k

Magnitude s
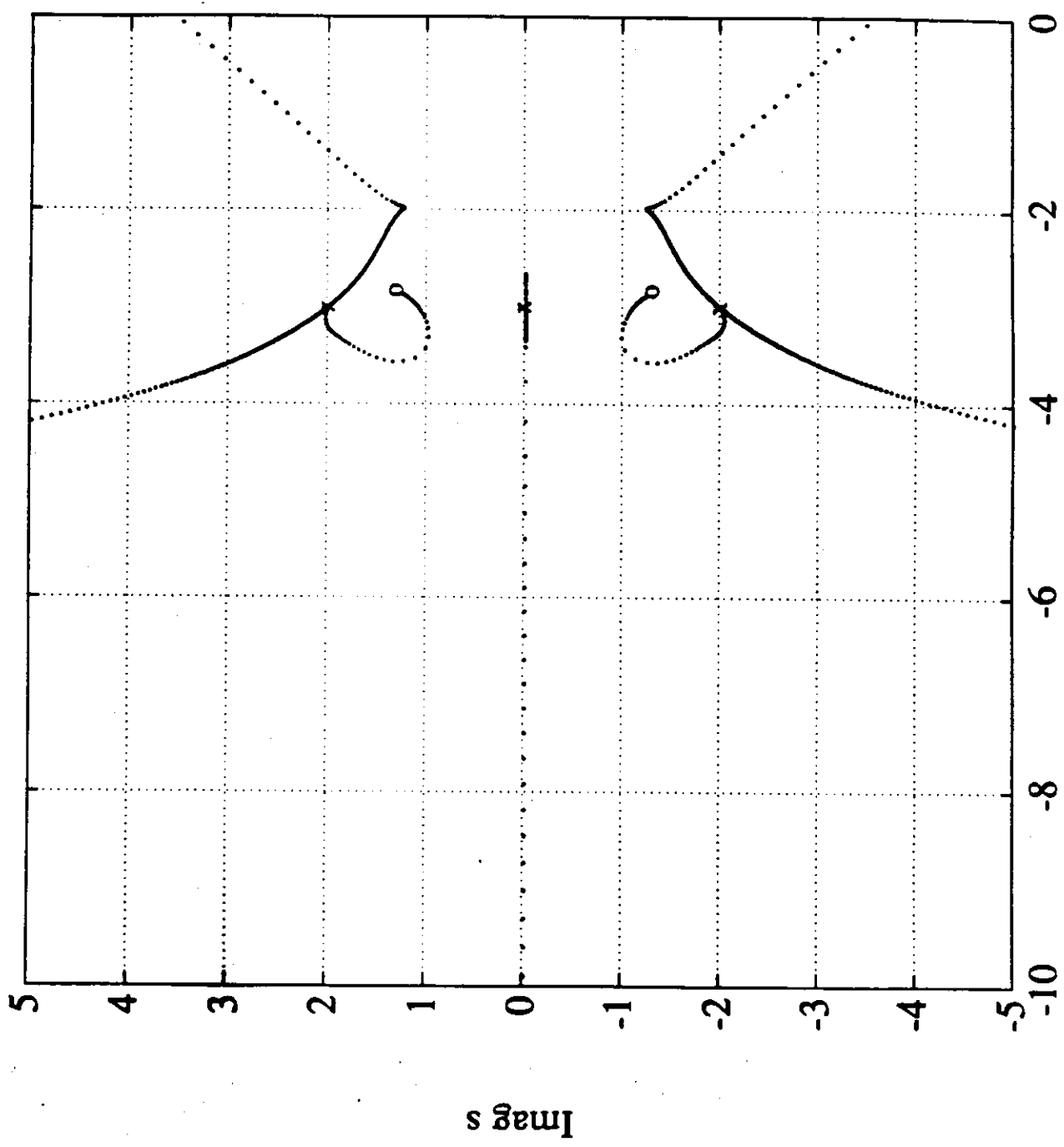
Magnitude k

FIG 6a

Angle of s vs Magnitude of k

Imag s

Real s